GANIT *J. Bangladesh Math. Soc.* (ISSN 1606-3694) **37** (2017) 121-129

HEAT TRANSFER BEHAVIOUR INSIDE A SINUSOIDAL CAVITY USING WATER BASED TIO_2 NANOfluID

Goutam Saha
Department of Mathematics, University of Dhaka, Dhaka-1000, Bangladesh
E-mail: ranamath06@gmail.com

Received 05.06.2017 Accepted 02.11.2017

ABSTRACT

A numerical investigation is carried out to observe the augmentation of heat transfer because of the presence of TiO_2 nanofluid inside a sinusoidal cavity. In this study, upper and lower walls of the cavity are considered adiabatic, higher and lower temperature are maintained at left and right vertical walls respectively. Also, 2D contour of velocity and temperature with average heat transfer rate are presented and discussed. Our findings show that augmentation of heat transfer is feasible with the increase of concentrations of nanoparticles.

Keywords: Heat transfer; nanofluid; sinusoidal enclosure; Rayleigh number; concentrations.

1. Introduction

"In many practical applications, natural convection is the only feasible mode of cooling of the heat source. Further, the shape of the heat transfer surfaces influences the development of the boundary layer. Therefore, the investigation of thermal and fluid flow behaviors for different shapes of the heat transfer surfaces is necessary to ensure the efficient performance of the various heat transfer equipments" [1]. Moreover, many numerical investigations are performed on complex geometries of enclosures and also on sinusoidal cavities [2-14].

The physical geometry and the coordinate systems are shown in Fig. 1. It consists of a sinusoidal cavity of dimensions, $L \times L$. Also, left and right vertical walls are considered as hot and cold surfaces and the other horizontal walls are considered to be adiabatic. The range of Rayleigh numbers is considered to be 10^3 to 10^6 and nanoparticles concentration χ is varied from 0 to 15%. [15]

We observe that no investigation has been done on the behaviours of heat transfer filled with nanofluid inside a sinusoidal cavity. The goal of this work is to examine the behaviour of heat transfer inside a sinusoidal cavity. Results of the velocity and temperature fields will be presented graphically and the average Nusselt number will be shown in tabular form. In addition, a new correlation will be presented for the calculation of $\overline{Nu}$.

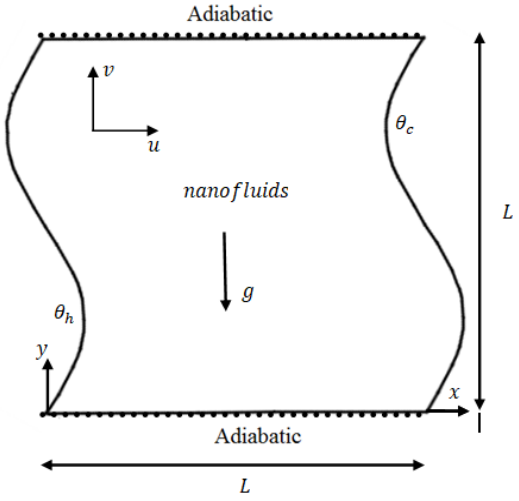

Fig. 1: Physical diagram

2. Mathematical Model

A steady state incompressible flow inside a sinusoidal cavity filled with water based TiO_2 nanofluid is considered in the present investigation. Moreover, the well known Navier-Stokes equations with the Boussinesq approximation are presented below:

$$\frac{\partial u_1}{\partial x_1} + \frac{\partial u_2}{\partial x_2} = 0 \tag{1}$$

$$u_1\frac{\partial u_1}{\partial x_1} + u_2\frac{\partial u_1}{\partial x_2} = -\frac{1}{\rho_{nf}}\frac{\partial p}{\partial x_1} + \nu_{nf}\left(\frac{\partial^2 u_1}{\partial {x_1}^2} + \frac{\partial^2 u_1}{\partial {x_2}^2}\right) \tag{2}$$

$$u_1\frac{\partial u_2}{\partial x_1} + u_2\frac{\partial u_2}{\partial x_2} = -\frac{1}{\rho_{nf}}\frac{\partial p}{\partial x_2} + \nu_{nf}\left(\frac{\partial^2 u_2}{\partial {x_1}^2} + \frac{\partial^2 u_2}{\partial {x_2}^2}\right) + (\rho\beta)_{nf}\, g(\theta - \theta_c) \tag{3}$$

$$u_1\frac{\partial \theta}{\partial x_1} + u_2\frac{\partial \theta}{\partial x_2} = \alpha_{nf}\left(\frac{\partial^2 \theta}{\partial {x_1}^2} + \frac{\partial^2 \theta}{\partial {x_2}^2}\right) \tag{4}$$

where u_1 and u_2 indicates the velocities, p is the pressure, θ is the temperature.

Nanofluids density, thermal diffusivity and heat capacitance are given as [16, 17, 18]

$$\begin{aligned} \rho_{nf} &= (1-\chi)\rho_f + \chi\rho_s \\ \alpha_{nf} &= \left(\frac{\kappa}{\rho c_p}\right)_{nf} \\ \left(\rho c_p\right)_{nf} &= (1-\chi)\left(\rho c_p\right)_f + \chi\left(\rho c_p\right)_s \end{aligned} \tag{5}$$

Nanofluids dynamic viscosity is given as (Brinkman [19])

$$\mu_{nf} = \frac{\mu_f}{(1-\chi)^{2.5}} \tag{6}$$

Also, nanofluids thermal conductivity, κ_{nf} is given as (Maxwell [20])

$$\frac{\kappa_{nf}}{\kappa_f} = \frac{\left(\kappa_s + 2\,k_f\right) - 2\chi\left(\kappa_f - k_s\right)}{\left(\kappa_s + 2\,k_f\right) - \chi\left(\kappa_f - k_s\right)} \tag{7}$$

The boundary conditions are:

Vertical walls are hot and cold respectively.

Horizontal walls are adiabatic. (8)

Let us consider the following non-dimensional variables:

$$X_1 = \frac{x_1}{L}, X_2 = \frac{x_2}{L}, U_1 = \frac{u_1\,L}{\alpha_f}, U_2 = \frac{u_2\,L}{\alpha_f}, P = \frac{p\,L^2}{\rho_{nf}\alpha_f^2}, T = \frac{\theta - \theta_c}{\theta_h - \theta_c} \tag{9}$$

Then, the dimensionless non-linear equations can be expressed as

$$\frac{\partial U_1}{\partial X_1} + \frac{\partial U_2}{\partial X_2} = 0 \tag{10}$$

$$U_1\frac{\partial U_1}{\partial X_1} + U_2\frac{\partial U_1}{\partial X_2} = -\frac{\rho_f}{\rho_{nf}}\frac{\partial P}{\partial X_1} + \frac{\nu_{nf}}{\alpha_f}\left(\frac{\partial^2 U_1}{\partial {X_1}^2} + \frac{\partial^2 U_1}{\partial {X_2}^2}\right) \tag{11}$$

$$U_1\frac{\partial U_2}{\partial X_1} + U_2\frac{\partial U_2}{\partial X_2} = -\frac{\rho_f}{\rho_{nf}}\frac{\partial P}{\partial X_2} + \frac{\nu_{nf}}{\alpha_f}\left(\frac{\partial^2 U_2}{\partial {X_1}^2} + \frac{\partial^2 U_2}{\partial {X_2}^2}\right) + \frac{(\rho\beta)_{nf}}{\rho_{nf}\beta_f}\,Ra\,Pr\,T \tag{12}$$

$$U_1\frac{\partial T}{\partial X_1} + U_2\frac{\partial T}{\partial X_2} = \frac{\alpha_{nf}}{\alpha_f}\left(\frac{\partial^2 T}{\partial {X_1}^2} + \frac{\partial^2 T}{\partial {X_2}^2}\right) \tag{13}$$

The corresponding boundary conditions for the above problem are given by:

All walls: $U_1 = U_2 = 0$, left side wall: T = 1 and right side wall: T = 0

Top and bottom walls: $\frac{\partial T}{\partial X_2} = 0$

Also, the local and average Nusselt number are defined as

$$Nu = -\frac{k_{nf}}{k_f}\frac{\partial T}{\partial X_1} \qquad \overline{Nu} = \int_{heated\ wall} Nu\,dX_2 \tag{14}$$

3. Numerical Procedure

It is really difficult to find the exact solution of non-dimensional PDEs with given boundary conditions. Therefore, an iterative scheme named FEM is considered in order to find the approximate solution of the given physical geometry. Moreover, six nodded triangular elements are considered throughout this investigation and TOL is considered as 10^{-8}. Details of the finite element formulation are described in [1].

4. Results and Discussion

In this research, variation of velocity and temperature profiles with different Ra and χ inside a sinusoidal cavity are presented in Figs. 2–3. Besides, variation of average Nusselt number is also presented in Fig. 4. In this study, range of parameters such as Ra and χ are considered as $10^3 \leq Ra \leq 10^6$ and $0 \leq \chi \leq 15\%$ respectively. In addition, properties of different types of fluids are presented in Table 1.

Moreover, grid independence test is carried out for different Ra and lots of simulations have been performed in order to assess the grid distribution. It is found that non-uniform grid of 5044 elements is sufficient to capture the correct profiles of velocity and temperature distributions inside a sinusoidal cavity. Details of the results are given in Table 2. Also, a comparison has been done for different Ra with previous works as well as benchmark results as shown in Table 3. It is found that present solutions are in good agreement with the other published works.

Table 1: Properties of the water and TiO_2 nanoparticles [21, 22]

Pr = 6.2	Fluid Phase	Solid Phase
Properties	Water, 300 K	TiO_2
μ (Ns/m^2)	8.55×10^{-4}	
C_p(J/Kg K)	4179	686.2
ρ (Kg/m^3)	997.1	4250
κ (W/m K)	0.613	8.9538
β (K^{-1}) $\times10^{-5}$	21	0.9
α (m^2/s) $\times10^{-5}$		0.31

Table 2: Grid independency test (Ra = 10^6 and χ = 0.01)

Elements	2822	2948	3790	4206	4934	5044
$\overline{Nu}$	5.58885	5.59914	5.50789	5.53774	5.54939	5.549931

Table 3: Code validation works

Ra	Present	Barakos and Mitsoulis [23]	Markatos and Pericleous [24]	De Vahl Davis [25]	Fusegi *et al.* [26]
10^3	1.118	1.114	1.108	1.118	1.105
10^4	2.244	2.245	2.201	2.243	2.302
10^5	4.515	4.510	4.430	4.519	4.646
10^6	8.789	8.806	8.754	8.799	9.012

Variation of streamline and isotherm profiles with different Rayleigh number for χ = 0.15 have been presented in Fig. 2. It is seen that flow moves along the clockwise pattern. It suggests that nanofluid particles inside the cavity moves up along the heated surface and then blocks at the adiabatic upper surface and then going down along the cooled surface and then moves towards the bottom adiabatic surface.

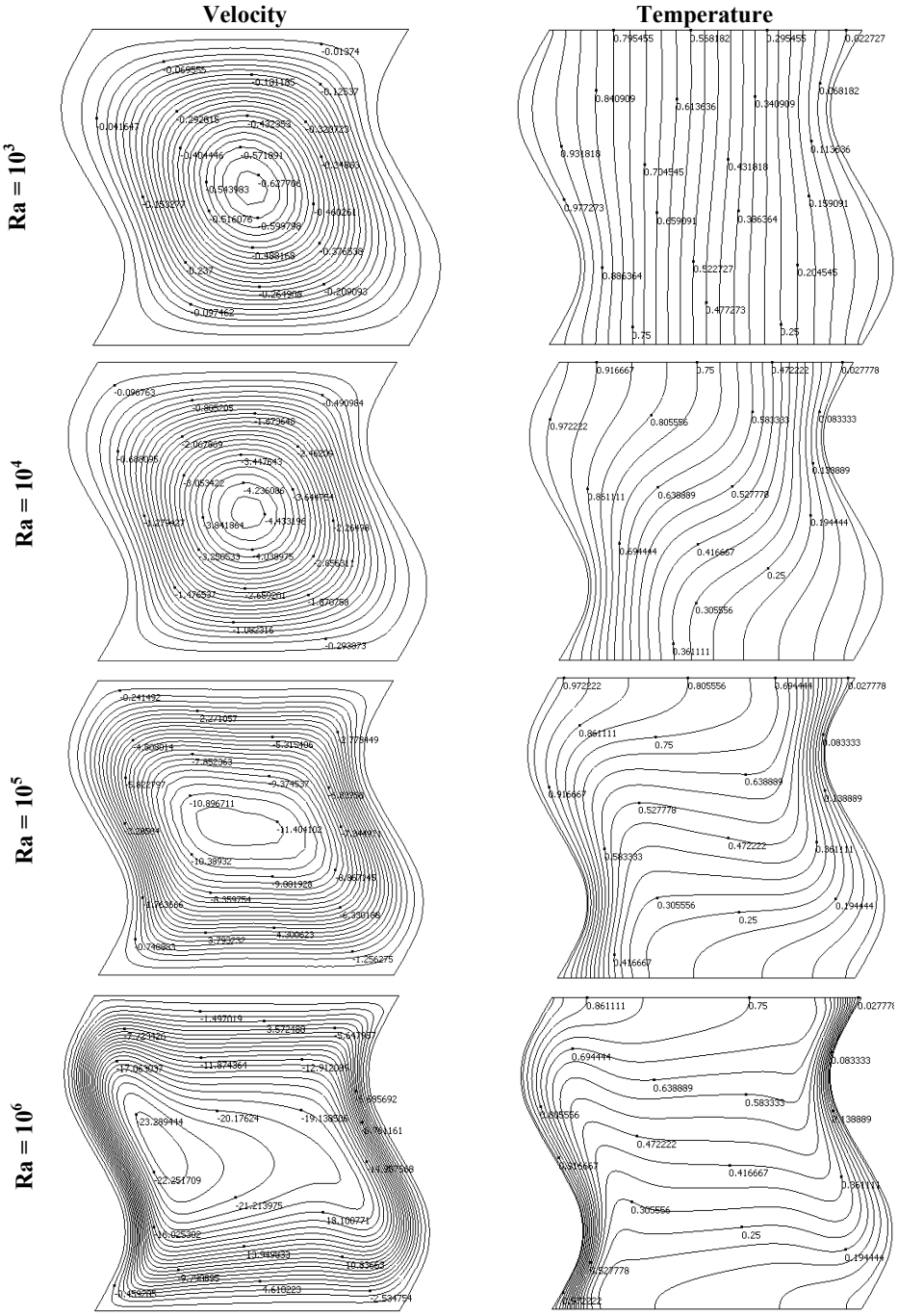

Fig. 2: Variation of velocity and temperature for $\chi = 0.15$

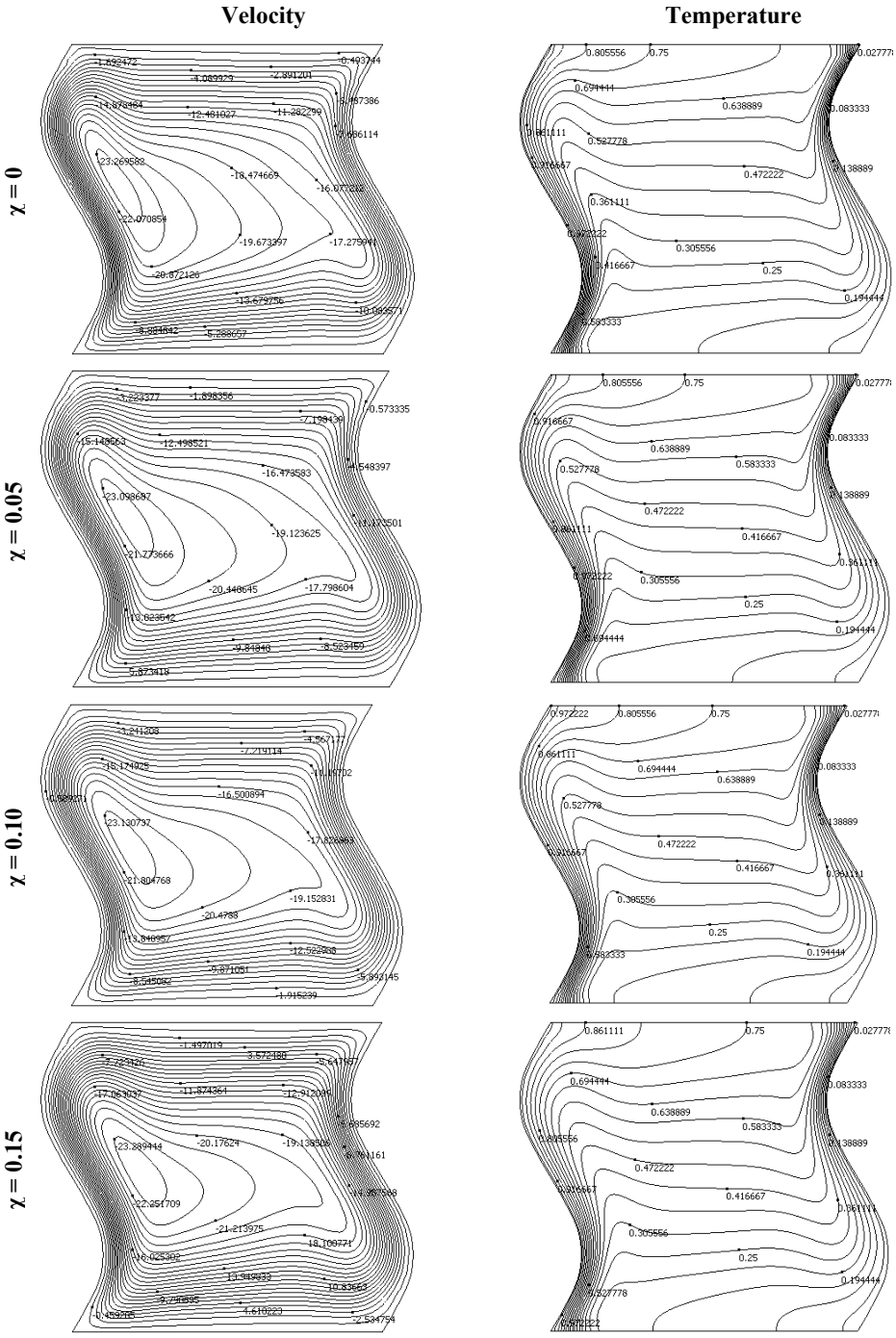

Fig. 3: Variation of velocity and temperature for various χ and $Ra = 10^6$

As shown in the Fig. 2, a single vortex is developed at low Ra. Also, the pattern of the central vortex is round in shape and it tends to become ellipsoidal with the increasing of Ra and in the end, central vortex moves near the left side wall and some deformations can be seen near the central zone for $Ra = 10^6$. It is to be noted that nanoparticles inclusion in the fluid affects the development of the vortex inside the cavity. Moreover, the strength of the flow circulation is superior with the increase of Ra when nanoparticles presence in the fluid taken is under consideration. It is due to the effect of nanoparticles concentrations as well as buoyancy force. Also, the temperature profile seems to be developed as a parallel layer along the vertical direction for low Ra. And, it tends to move towards the wall region with the increase of Ra and some horizontal layers are developed inside the centerline area of the cavity. This is also due to effect of buoyancy force.

Variation of streamline and isotherm profiles with different nanoparticles concentrations for Ra = 10^6 have been presented in Fig. 3. It is found that elliptical shape centrally concentrated vortex is formed and developed towards the heated wall region for different concentrations. It is also found that in the absence of nanoparticles and for high $Ra = 10^6$, several vortex near the heated wall emerge as a leading attribute of the flow field. Also, the flow movement inside the cavity remains similar as discussed in Fig. 2. Moreover, as the nanoparticles concentrations increases, streamlines pattern seems to be squeezed at the central line position and dense near the boundaries. It is to be noted that maximum nanofluid velocity is also increased with the increase of concentrations. It is due to the higher nanoparticles concentration which helps to increase the thermal conductivity of nanofluids. This leads to the augmentation of energy which forces to speed up the flow. However, isotherm pattern seems to be similar to the previous results as shown in Fig. 2.

5. Heat Transfer Correlation

A new correlation has been proposed to calculate the average Nusselt number along the heated surface for $10^3 \leq Ra \leq 10^6$ and $0 \leq \chi \leq 0.15$. And the correlation is presented below:

$$\overline{Nu} = a\,(1 + \chi^n)Ra^m$$

where $a = 0.0783763,\ n = 1.587369,\ m = 0.3081744$ and $R^2 = 99.9\%$.

Table 4: Avg. Nusselt number, $\overline{Nu}$ for different Ra and χ

Ra	$\chi = 0$	1%	2%	3%	4%	5%	6%	7%
					$\overline{Nu}$			
10^3	0.649383	0.659271	0.669661	0.680562	0.702618	0.703909	0.716358	0.729323
10^4	1.287573	1.292638	1.297321	1.301619	1.361167	1.309037	1.312154	1.314874
10^5	2.694997	2.707888	2.720044	2.73147	2.853908	2.752137	2.761387	2.769921
10^6	5.448933	5.479941	5.50957	5.537847	5.780716	5.590425	5.614761	5.637811
Ra	8%	9%	10%	11%	12%	13%	14%	15%
					$\overline{Nu}$			
10^3	0.742802	0.756792	0.771291	0.786295	0.8018	0.817804	0.834303	0.851297
10^4	1.317204	1.319146	1.320714	1.321921	1.322788	1.323343	1.323618	1.323656
10^5	2.77775	2.784877	2.791314	2.797071	2.802156	2.806581	2.810357	2.813493
10^6	5.659589	5.680095	5.699341	5.717328	5.734055	5.749523	5.763728	5.776663

Moreover, variation of average Nusselt number with different *Ra* has been presented in Table 4. It is seen that heat transfer rate increases with the increase of *Ra*. It is evident that the values of $\overline{Nu}$ increase as *Ra* increases from 10^3 to 10^6 for all values of nanoparticles concentrations.

Conclusion

Flow and heat transfer behaviours of nanofluid inside a 2D sinusoidal cavity have been presented and discussed for different Ra and χ. Also, variation of streamlines and isotherms for a wide range of Ra and χ were presented graphically. Our findings reveal that heat transfer augmentation is possible using TiO_2 nanofluid and such heat transfer rate is found higher compared with base fluid water. Moreover, nanoparticles concentrations have significant effect on the flow field, specially for high Ra.

REFFERENCES

[1] G. Saha, Finite Element Simulation of Magnetoconvection Inside a Sinusoidal Corrugated Enclosure with Discrete Isoflux Heating From Below**,** *Int. Comm. Heat Mass Transfer* **37(4)** (2010) 393-400.

[2] S. Mahmud, P.K. Das, N. Hyder, A.K.M.S. Islam, Free convection in an enclosure with vertical wavy walls, *Int. J. Thermal Sci.* **41** (2002) 440-446.

[3] S. Mahmud, R.A. Fraser, Visualizing energy flows through energy streamlines and path lines, *Int. J. Heat Mass Transfer* **50** (2007) 3990-4002.

[4] Z. Sultana, N. Hyder Md., Non-darcy free convection inside a wavy enclosure, *Int. Comm. Heat Mass Transfer* **34** (2007) 136-146.

[5] P.K. Das, S. Mahmud, Numerical investigation of natural convection inside a wavy enclosure, *Int. J. Thermal Sci.* **42** (2003) 397-406.

[6] Y. Varol, H.F. Oztop, Free convection in a shallow wavy enclosure, *Int. Comm. Heat Mass Transfer* **33** (2006) 764-771.

[7] S. Abdelkader, R. Mebrouk, B. Abdellah and B. Khadidja, Natural convection in a horizontal wavy enclosure, *J. Appl. Sci.* **7** (2007) 334-341.

[8] K. Khanafer, B. Al-Azmi, A. Marafie, I. Pop, Non-Darcian effects on natural convection heat transfer in a wavy porous enclosure, *Int. J. Heat Mass Transfer* **52** (2009) 1887-1896.

[9] L. Yao, Natural convection along a vertical wavy surface, *J. Heat Transfer* **105** (1983) 465-468.

[10] S. Saha, T. Sultana, G. Saha, M. Rahman, Effects of discrete isoflux heat source size and angle of inclination on natural convection heat transfer flow inside a sinusoidal corrugated enclosure, Int. Comm. *Heat Mass Transfer* **35** (2008) 1288-1296.

[11. M. Sheikholeslami, H.F. Oztop, MHD free convection of nanofluid in a cavity with sinusoidal walls byusing CVFEM, *Chinese Journal of Physics* (2017) (Accepted).

[12] W. Tang, M. Hatami, J. Zhou, D. Jing, Natural convection heat transfer in a nanofluid-filled cavity with doublesinusoidal wavy walls of various phase deviations, *Int. J. Heat Mass Transfer* **115** (2017) 430-440.

[13] M. Sheikholeslami, H.B. Rokni, Influence of EFD viscosity on nanofluid forced convection in a cavitywithsinusoidal wall, *J. Molecular Liquids* **232** (2017) 390–395.

[14] M. Sheikholeslami, M. Gorji-Bandpy, D.D. Ganji, .S. Soleimani, Natural convection heat transfer in a cavity with sinusoidal wall filled with CuO–water nanofluid in presence of magnetic field, *J. Taiwan Institute Chemical Engineers* **45** (2014) 40-49.

[15] R.J. Issa, Effect of Nanoparticles Size and Concentration on Thermal and Rheological Properties of AL_2O_3-Water Nanofluids, Proceedings of the World Congress on Momentum, *Heat and Mass Transfer* (MHMT'16) Prague, Czech Republic – April 4-5, 2016 Paper No. ENFHT 101.

[16] G. Saha, M.C. Paul, Numerical analysis of heat transfer behaviour of water based Al_2O_3 and TiO_2 nanofluids in a circular pipe under the turbulent flow condition, *Int. Comm. Heat Mass Transfer*, **56** (2014) 96-108.

[17] G. Saha, M.C. Paul, Heat transfer and entropy generation of turbulent forced convection flow of nanofluids in a heated pipe, Int. Comm. *Heat Mass Transfer*, 61 (2015) 26-36.

[18] G. Saha, M.C. Paul, Transition of Nanofluids Flow in an Inclined Heated Pipe, *Int. Comm. Heat Mass Transfer*, **82** (2017) p. 49-62.

[19] H.C. Brinkman, The viscosity of concentrated suspensions and solutions, *J. Chem. Phys.* **20** (1952) 571-581.

[20] J. Maxwell, A Treatise on Electricity and Magnetism, second ed. Oxford University Press, Cambridge, UK, 1904.

[21] E. Abu-Nada, Z. Masoud, A. Hijazi, Natural convection heat transfer enhancement in horizontal concentric annuli using nanofluids, *Int. Comm. Heat Mass Transf.* **35** (5) (2008) 657-665.

[22] E. Abu-Nada, A.J. Chamkha, Effect of nanofluid variable properties on natural convection in enclosures filled with a CuO-EG-Water nanofluid, *Int. J. Thermal Sciences*. **49** (2010) 2339-2352.

[23] G. Barakos, E. Mitsoulis, Natural convection flow in a square cavity revisited: laminar and turbulent models with wall functions, *Int. J. Numer. Methods Fluids* **18** (1994) 695-719.

[24] N.C. Markatos, K.A. Pericleous, Laminar and turbulent natural convection in an enclosed cavity, *Int. J. Heat Mass Transfer* **27** (1984) 772-775.

[25] G.D.V. Davis, Natural convection of air in a square cavity, a benchmark numerical solution, *Int. J. Numer. Methods Fluids* **3** (1962) 249-264.

[26] T. Fusegi, J.M. Hyun, K. Kuwahara, B. Farouk, A numerical study of three-dimensional natural convection in a di□erentially heated cubical enclosure, *Int. J. Heat Mass Transfer* **34** (1991) 1543-1557.